Rheol Acta (2002) 41: 103–113

ORIGINAL CONTRIBUTION

Stefan Trinkle
Philipp Walter
Christian Friedrich

Van Gurp-Palmen Plot II – classification of long chain branched polymers by their topology

Received: 17 April 2001
Accepted: 20 June 2001

S. Trinkle · P. Walter · C. Friedrich (✉)
Institut für Makromolekulare Chemie
Albert Ludwig Universität Freiburg
Stefan-Meier Str. 31
79109 Freiburg i. Br., Germany
e-mail: chf@fmf.uni-freiburg.de

Abstract Rheological data on monodisperse model-type polymers with a certain topology are available in the literature. A comparison between these series has not been made yet, mainly because the different chemical nature of these polymers inhibited a direct comparison. With the so-called reduced van-Gurp-Palmen plot (rvGP) this task has become possible and this article applies this plot to these model-type polymers. We check whether these polymers exhibit features allowing one to classify them on basis of the corresponding linear viscoelastic data. We define a characteristic point $P_C(G_{red,c}, \delta_c)$ that represents the sample. By drawing all available points in rvGP-coordinates we obtain a topology map on which certain topologies cover distinct areas on this map. Unfortunately these areas overlap to some extent. For the unambiguous characterization of an unknown sample additional information is needed.

We apply the topology map to metallocene poly(olefin)s.

Key words Rheology · van Gurp-Palmen plot · Topology map · Long chain branching · Metallocene poly(olefin)s

Introduction

Many research groups are concerned with the quantitative characterization of long chain branching (LCB) in polymeric materials. This is not an easy task since one of the major problems is the low number of branching points along the chain and thus a low branching point density. For this reason, the spectroscopic methods fail to work; at least, the corresponding results are erroneous quantities. Rheology, however, is in the meanwhile the accepted method of choice, since the introduction of even low levels of LCB to a linear polymer results in a significant change in the flow behavior. Rheology alone is unfortunately ambiguous. So, the LCB indexes based solely on rheology like the Dow Rheology (Lai et al. 1994) and the Activation Energy-Index (Vega and Santamaria 1998) are overruled (Seo and Ung Kim 1994; Shroff and Mavridis 1999; Wood-Adams and Dealy 2000) and extended or replaced by techniques combining two analysis methods. For example, Shroff and Mavridis (1999) as well as Janzen and Colby (1999) couple the information from melt rheology and solution viscometry and get a quantity that is a measure of the branching level. Wood-Adams and Dealy (1996, 2000) and Wood-Adams et al. (2000) as well as Shaw and Tuminello (1994) use rheology and Size Exclusion Chromatography (SEC) as their method. These studies focus on the number of branching points. However, even more important is the location of the branching point along the chain backbone that determines the polymer's topology. There are some studies on different polymers investigating different types of well-defined topologies (Gell et al. 1997a, b; Fetters et al. 1993; McLeish et al. 1999; Roovers 1979; Roovers and Toporowski 1981; Roovers and Graessley 1981) but the question whether there are characteristic fingerprints for these different types of topologies remains open. Two reason account for this. First, the number of available data sets is limited because of the complex synthesis pathways and, second, the polymers of each topology class series are of

different chemical natures so a comparison between two series is or was not possible. At this point the reduced van Gurp-Palmen plot (rvGP) (Trinkle and Friedrich 2001) provides a solution since it allows sketching of the data of different samples directly in one figure regardless of their chemical constitution. Consequently, the concern of this article is to check if there exist fingerprints characteristic of a certain topology. This is one step in the endeavor to establish a satisfactory method for the characterization of long chain branching based on the linear viscoelastic properties of a sample.

Because presentation of rheological data in the reduced van Gurp-Palmen plot (rvGP) is novel, important, and yet sparsely applied, we will first briefly summarize the features of linear polymers and then turn to certain long chain branched model polymers. During the course of the article we systematically focus on rheological data of these model substances that have been synthesized and published by other scientist (Gell et al. 1997a, b; Fetters et al. 1993; McLeish et al. 1999; Roovers 1979; Roovers and Toporowski 1981; Roovers and Graessley 1981). From model series to model series the number of side arms increases. We start with one side arm attached to a backbone, namely three-arm stars, turn then to four-arm stars, go over to H-shaped polymers with two side chains that are attached to the backbone at different locations, however, and end with comb-polymers having approximately 30 side arms. Finally, we show the rvGP-plots of technically important metallocene type poly(olefin)s, that are less homogenous by means of their branching structure, arm lengths, and molecular weight distribution.

Experimental

Materials

Asymmetric stars The asymmetric three-arm star polymers were poly(ethene-*alt*-propene)s. Within this series, the backbone M_w was kept nearly constant and the length of the side arm was increased gradually. The synthesis, characterization and rheological measurements were published by Gell et al. (1997a, b) and the characteristic quantities are given in Table 1.

Symmetric stars The symmetric four-arm star polymers were poly(isoprene)s with varied arm lengths and thus varied entire molecular weights. The synthesis, characterization, and rheological data were published by Fetters et al. (1993) and the characteristic quantities are given in Table 2.

H-shaped polymers Rheological data of two different series of H-polymers are under investigation in this manuscript. First, weakly entangled poly(styrene)s with equal arm- and crossbar molecular weights. Within this series, the total molecular weight was increasing. Second, highly entangled poly(isoprene)s with varied geometry ratios. Synthesis, characterization, and rheological data of the first series were published by Roovers and Toporowski (1981) and Roovers (1984). Synthesis, characterization, and rheological properties of the remaining Hs are covered by a publication by McLeish et al. (1999). The characteristic data are given in Tables 3 and 4. For reasons of correspondence, we have adapted McLeish's corrected values for the molecular weights s_{arm} and s_{bb}.

Comb polymers Two series of poly(styrene) comb polymers were included in this work. The polymers of the two rows differ in the backbone molecular weight and within each series the lengths of the side arms were increased gradually. The number of branches was kept constant (approximately 30). Synthesis, characterization, and rheological data are published by Roovers (1979) and Roovers and Graessley (1981). The characteristic parameters are provided in Table 5.

Nomenclature Each polymer is thought to be built up by a backbone and attached side arms. For star-polymers, which actually do not have any backbone at all, the two longest side arms are considered to be the backbone and the remaining arms are thought to be the *side* arms. The cross bar of an H-shaped molecule is taken as the backbone and the four arms are the *side* arms. The model polymers are coded throughout this paper in a uniform manner by three information units: (i) topology type; aS for asymmetric star, sS for symmetric star, H for H-shaped molecules and C for comb polymers, (ii) molecular weight of backbone, respectively molecular weight of cross bar in case of Hs, and (iii) molecular weight of side arms. The molecular weights are expressed in multiples of the corresponding entanglement molecular weight, i.e., s_{bb} (bb = backbone) and s_{arm}. s_{bb} and s_{arm} are separated by a dash. The indexed letter s denotes the number of entanglements of the corresponding chain element.

Table 1 Asymmetric three-arm star-shaped poly(ethylene-*alt*-propylene) by Gell et al.

Code	Crossbar M_w[a] [kg/mol]	Arm M_w[a] [kg/mol]	#Arms	M_w/M_n	Entire M_w[a] [kg/mol]	G_N^0[b] [Pa]	M_{arm}/M_{bb}	$S_{arm} = M_{arm}/M_e$	$S_{bb} = M_{bb}/M_e$	Original name
aS38-0	88	–	3	No data reported anionic polym.	88	1.0×10^6	0	0	38.3	S00
aS39-0.5	90	1.1			91	1.28×10^6	0.012	0.5	39.1	S01
aS42-2.4	96	5.5			102	1.40×10^6	0.057	2.4	41.7	S06
aS35-7.4	80	17.0			97	1.65×10^6	0.213	7.4	34.8	S17
aS37-18	84	42.0			126	1.44×10^6[c]	0.5	18.3	36.5	S42

Data taken from Gell et al. (1997a, b)
M_e = 2300 g/mol as reported by Gell et al. (1997a, b)
[a] M_w data obtained by LALLS. M_{bb} and M_{arm} are the M_w of the precursors
[b] G_N^0 determined by $G_N^0 = |G^*|$ in minimum (Trinkle and Friedrich 2001)
[c] Mean value of G_N^0 of aS39-0.5, aS42-2.4 and aS35-7.4

Table 2 Symmetric four-arm star-shaped poly(isoprene)s by Fetters et al.

Code	Back bone M_w [kg/mol]	Arm M_w [kg/mol]	#Arms	M_w/M_n	Entire M_w [kg/mol]	$G_N^{0\,a}$ [Pa]	M_{arm}/M_{bb}	$s_{arm} = M_{arm}/M_e$	$s_{bb} = M_{bb}/M_e$	Original name
sS100-0	500	–	0	No data reported anionic polym.	500	4×10^5	–	–	100	Lin500
sS6.8–3.4	34	17.0	4		68	4×10^5	0.5	3.4	6.8	68K
sS15-7.3	73	36.7	4		148	4×10^5		7.3	14.6	148K
sS19-9.5	95	47.5	4		188	4×10^5		9.5	19.0	188K
sS29-14	144	72.2	4		280	4×10^5		14.4	28.8	280K
sS38-19	190	95.0	4		380	4×10^5		19.0	38.0	380K

Data as reported by Fetters et al. (1993)
M_e = 5000 g/mol by Fetters et al. (1993)
[a] G_N^0 taken from Donth (1992)

Table 3 H-shaped poly(isoprene)s by McLeish et al.

Code	Crossbar M_w [kg/mol]	Arm M_w [kg/mol]	#Arms	M_w/M_n	Entire M_w [kg/mol]	$G_N^{0\,d}$ [Pa]	M_{arm}/M_{bb}	$S_{arm}{}^e$	$s_{bb}{}^e$	$\phi_{arm}{}^f$	$\phi_{bb}{}^g$	Original name
H29-5.2	111[a]	20.0[a]	4	1.1	198[a]	4×10^5	0.18	5.2	28.9	0.42	0.58	H1I0B20
H21-10	111[a]	52.5[a]	4	1.1	310[a]	4×10^5	0.47	10.4	22.2	0.65	0.35	H1I0B52
H25-9.4	164[b]	40.0[b]	4	1.1	324[c]	4×10^5	0.25	9.4	25.2	0.60	0.40	H160B40
H34-16	198[b]	63.0[b]	4	1.3	460[c]	4×10^5	0.32	16.0	34.0	0.59	0.41	H200B65

Data as reported by McLeish et al. (1999)
[a] M_w determined by membrane osmometry
[b] M_w determined by SEC
[c] M_w determined by LALS
[d] G_N^0 taken from Donth (1992)
[e] s_{arm} and s_{bb} were taken from McLeish et al. (1999), who corrected s_{arm}/s_{bb} individually to fit best the experimental data
[f] $\phi_{arm} = 4s_{arm}/(4s_{arm} + s_{bb})$
[g] $\phi_{bb} = s_{bb}/(4s_{arm} + s_{bb})$

Table 4 H-shaped poly(styrene)s by Roovers and Toporowski

Code	Crossbar $M_w{}^a$ [kg/mol]	Arm $M_w{}^a$ [kg/mol]	#Arms	M_w/M_n	Entire $M_w{}^b$ [kg/mol]	$G_N^{0\,c}$ [Pa]	M_{arm}/M_{bb}	$s_{arm} = M_{arm}/M_e$	$s_{bb} = M_{bb}/M_e$	$\phi_{arm}{}^d$	$\phi_{bb}{}^e$	Original name
H2.4-2.5	44	46	4	No data reported anionic polymerization	237	2.33×10^5	1.0	2.5	2.4	0.8	0.2	H2A1
H5.5-5.7	100	103	4		483	1.88×10^5		5.7	5.5	0.8	0.2	H1A1
H11-11	204	205	4		1 040	1.98×10^5		11.3	11.3	0.8	0.2	H5A1
H1.1-1.1	19	19.3	4		111	2.58×10^5		1.1	1.1	0.8	0.2	H4A1A
H6.8-7.3	123	132	4		674	2.13×10^5	1.1	7.3	6.8	0.8	0.2	H3A1
H46-0	830	–	0		830	2.13×10^5	–	–	46	0	1	PS830

Data taken from Roovers and Toporowski (1981)
Me = 18 000 g/mol by Donth (1992)
[a] M_w of crossbar and arms: data of precursors
[b] Entire M_w by light scattering in cyclohexane
[c] Determined by means of δ_{min} in the vGP-plot
[d] $\phi_{arm} = 4s_{arm}/(4s_{arm} + s_{bb})$
[e] $\phi_{bb} = s_{bb}/(4s_{arm} + s_{bb})$

Poly(olefin)s These polymers were metallocene ethene/olefin copolymers of different molar masses and typical polydispersities between 2 and 2.5. The synthesis and characterization of the considered samples are described in detail elsewhere (Suhm 1998; Walter 2000). The polymers were stabilized with antioxidants against thermal degradation, chain extension, and/or scissoring, respectively. The determination of the plateau moduli, G_N^0, for the ethene/1-olefin copolymers is discussed in our preceding article (Trinkle and Friedrich 2001). The molecular weights are given in Table 6.

Polymer blend: linears/LCB Mixtures of sample mPE07 – a long chain branched poly(ethene) – and linear poly(ethene) with a similar polydispersity index were solution blended. The weight-ratio between LCB- and linear components was varied. The polymers were stabilized with antioxidants against thermal degradation.

Table 5 Comb-shaped poly(styrene)s by Roovers and Graessley

Code	Crossbar M_w[a] [kg/mol]	Arm M_w[a] [kg/mol]	#Arms	M_w/M_n	Entire M_w[a] [kg/mol]	G_0^N [Pa][c]	M_{arm}/M_{bb}	$s_{arm} = M_{arm}/M_e$	$s_{bb} = M_{bb}/M_e$	ϕ_{arm}[b]	ϕ_{bb}[c]	Original name
C15-0	275	–	–	< 1.06	275	2.05×10^5	0	0	15.3	0	1	C6bb
C15-1.4	275	25.7	25	< 1.06	913	2.5×10^5[d]	0.09	1.4	15.3	0.70	0.30	C632
C15-2.6	275	47.0	29	< 1.06	1 630	2.1×10^5	0.17	2.6	15.3	0.83	0.17	C642
C15-5.4	275	98.0	29	< 1.06	3 130	2.2×10^5	0.35	5.4	15.3	0.91	0.09	C652
C48-0	860	–	–	< 1.06	860	2.1×10^5	0	0	47.8	0	1	C7bb
C48-1.4	860	25.7	26	< 1.06	1 530	1.95×10^5	0.30	1.4	47.8	0.43	0.57	C732
C48-2.6	860	47.0	29	< 1.06	2 230	2.0×10^5	0.05	2.6	47.8	0.61	0.39	C742

Data taken from original literature (Roovers 1979; Roovers and Graessley 1981)
M_e = 18, 000 g/mol taken from Donth (1992)
[a] M_w data obtained by Light scattering
[b] ϕ_{arm} = #branches × s_{arm}/(#branches × s_{arm} + s_{bb})
[c] ϕ_{bb} = s_{bb}/(#branches × s_{arm} + s_{bb})
[d] Corrected from van-Gurp-Palmen-plot

Table 6 Characteristic data of the poly(olefin)s which are ethene/propene copolymers with different contents of propene

Code	M_n [kg/mol]	M_w [kg/mol]	wt% propene	M_w/M_n
mPE01	63	170	89	2.7
mPE02	78	195	10	2.5
mPE03	62	155	24	2.5
mPE04	189	642	0	3.4
mPE05	105	178	30	1.7
mPE06	152	258	17	1.7
mPE07	32	64	0	2.0

M_n and M_w by SEC

Rheology

The rheological data of the model stars, H-shaped polymers, and combs were taken from the literature. The rheological data of the metallocene poly(olefin)s were obtained with the Bohlin CVO 120 rheometer equipped with 25-mm parallel plate geometry. The applied stresses were within the limits of linear viscoelasticity. Isothermal frequency sweeps were recorded at varied temperatures within $10^{-2} < \omega < 10^2$ rad/s. In case of the LCB-linear polymer blend, the isotherms were shifted along the abscissa obtaining master curves. Since the time temperature superposition principle does not hold with LCB resins, only the isotherm at $T_{ref} = 170$ °C was taken for further analysis for the remaining samples. In order to determine the long time viscoelastic behavior of the samples, creep measurements were performed at 170 °C. The creep data were converted into the retardation time spectrum $L(\tau)$ by the computer program *NLReg* (Honerkamp and Weese 1993a). Subsequently, the complex shear compliance $J^*(\omega)$ was calculated from $L(\tau)$ (Honerkamp and Weese 1993b) and the shear moduli G' and G'' from $J^*(\omega)$. The obtained curves were superimposed with the 170 °C isotherm (Fig. 1). With this procedure of combining oscillatory and creep measurements, master curves can be extended towards lower frequencies (Trinkle and Friedrich 2001; Eckstein et al. 1998).

Results and discussion

Before turning to long chain branched (LCB) polymers, we want to summarize briefly the characteristics of linear polymers in the van Gurp-Palmen-plot (Trinkle and Friedrich 2001). Here, rheological data are shown by plotting the phase angle, δ, between stimulus and material response vs the absolute value of the complex modulus, $|G^*|$. The van Gurp-Palmen plot is temperature invariant and provides a method to check for the time temperature superposition principle (van Gurp and Palmen 1998). In the non-reduced form the curve of a linear polymer passes a minimum at G_N^0, raises up passing a point of inflection, and goes over into a plateau at 90° when going from high to low $|G^*|$-values – see poly(styrene) in Fig. 2. Replacing $|G^*|$ by the quotient $|G^*|/G_N^0$ results in the reduced van Gurp-Palmen plot (rvGP) and features such as chemical constitution, tacticity, and monomer composition in copolymers do not influence the curve any more. The molecular weight (MW) of a sample can be seen in the height of the G_N^0 minimum: the higher MW, the lower δ in the minimum. Increasing the polydispersity index $PI = M_W/M_n$ results in flattened curves – see PS and PE in Fig. 2. It is

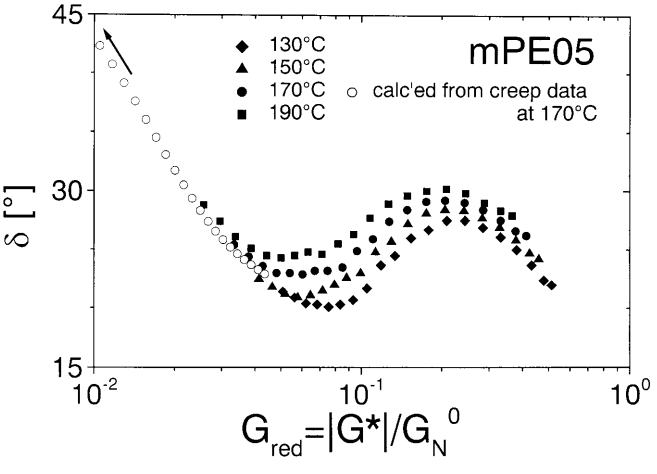

Fig. 1 Oscillatory measurements cover the upper frequency- and thus the upper G_{red} range and creep measurement extends the experimental window towards lower frequencies and G_{red}-values

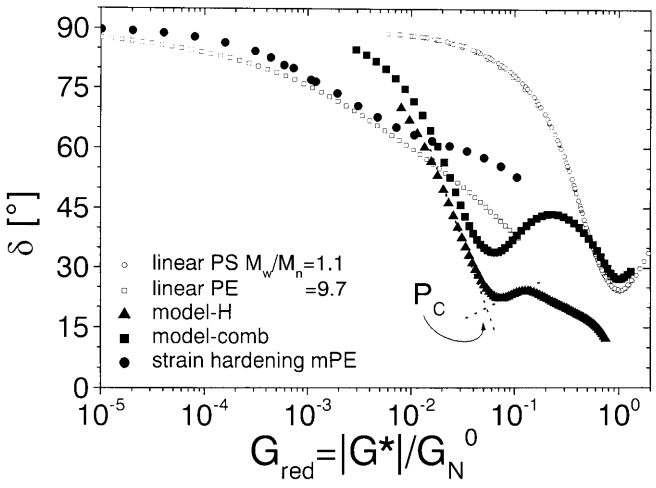

Fig. 2 The rvGP plot of linear poly(styrene)s and linear poly(ethene) with different polydispersity indices and three model LCB-polymers

important to notice that MW and PI do not change the type of curve – as discussed in detail in the preceding article (Trinkle and Friedrich 2001) – and the big advantage of the rvGP-plot is that it allows to compare directly two polymers of different chemical nature.

Figure 2 shows the van Gurp-Palmen plots, in the reduced or scaled form, of an H-shaped polymer, a comb, and a metallocene LLDPE along with two non-LCB polymers (''linears'') of different polydispersity index. The LCB topologies were ensured by a thought-out synthesis route. The metallocene LLDPE (Gabriel and Münstedt 1999) is a resin that shows strain hardening behavior under non-linear conditions. The literature regards strain hardening of being characteristic for long chain branched polymers. The message of Fig. 2 is that the LCB curves differ from the linear ones in the course of the curve and important in this context is the fact that the Size Exclusion Chromatography (SEC) verifies monomodality of these samples. In our previous article we showed that linear samples pass a minimum at $|G^*| = G_N^0$ in the van Gurp-Palmen plot, rise with decreasing $|G^*|$, G_{red} respectively, and finally reach the flow plateau at 90°. In contrast, the LCB samples have a more or less developed bump between the G_N^0 minimum and the 90° plateau. The two ''linear'' curves are substantially equal, i.e., both have one inflection point and do not exhibit any bump. The high polydispersity index of $M_w/M_n \approx 10$ accounts for the flattened curve but not for any bump.

Such an LCB bump is quantitatively described by a characteristic point P_c which is defined by the intersection of two tangent lines through the inflection points enclosing the bump as shown for the H-polymer in Fig. 2. P_c has two coordinates, $G_{red,c}$ and δ_c, and can be reliably determined if the polydispersity index M_W/M_n of the sample is below approximately 5. In the following the index ''c'' refers to a bump characterized by a point P_c. Before turning to industrially important poly(olefin)s, we focus in the next section on model LCB polymers.

Model-polymers

Asymmetric three-arm star-polymers

Three-arm stars can be regarded as the most simple long chain branched polymers. While two arms build up the backbone the third one is the side chain. Gell et al. (1997b) investigated a series of three-arm stars with nearly constant backbone and varied arm lengths. In the van Gurp-Palmen plot (Fig. 3) aS39–0.5 behaves very similarly to the linear aS38–0 owing to the fact that the side arm is too short to entangle ($s_{arm} < 1$). As s_{arm} exceeds unity, deviation from the linear behavior occurs and a bump at $G_{red} < 1$ develops. Starting from P_c at (1/0) of a hypothetical monodisperse linear polymer with $M_w = \infty$, this bump, characterized by the point P_c, moves up left with increasing arm length. There is no linear correlation between arm length (s_{arm}) and either coordinate of P_c.

Symmetric four-arm star-polymers

With this series of four-arm stars we have the same situation as with the three-arm stars (Fig. 4) except that the number of side arms is increased. The sample row comprises one linear polymer and stars with all four arms having the same length. The molecular weight of the arms and thus the entire M_w is varied. Similar to the three-arm

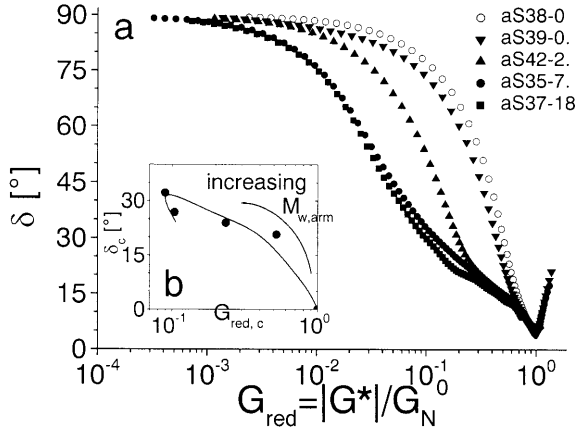

Fig. 3 a RvGP curves of asymmetric star–polymers (poly(ethene-*alt*-propene)) by Gell et al. at 100 °C. M_{bb} was kept constant at approximately 88 kg/mol and the length of the side arm was varied. **b** Location of points P_C, i.e., δ_c vs $G_{red,C}$

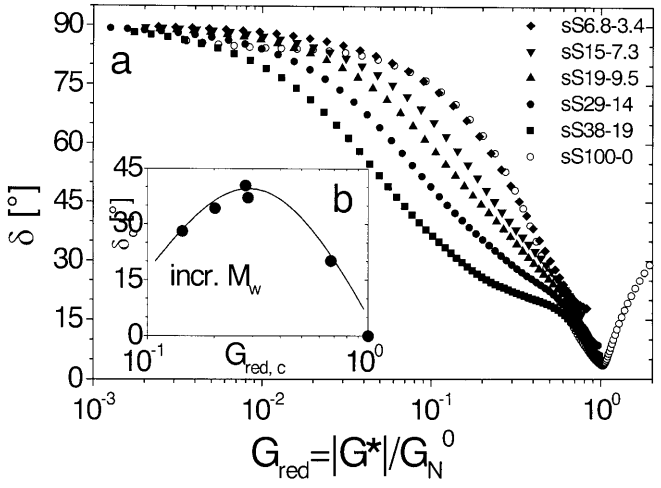

Fig. 4 a Symmetric four-arm star–poly(isoprene)s at 25 °C. s_{arm}:s_{bb} ratio was kept constant and total MW was varied. **b** Location of points P_C, i.e., δ_c vs $G_{red,C}$

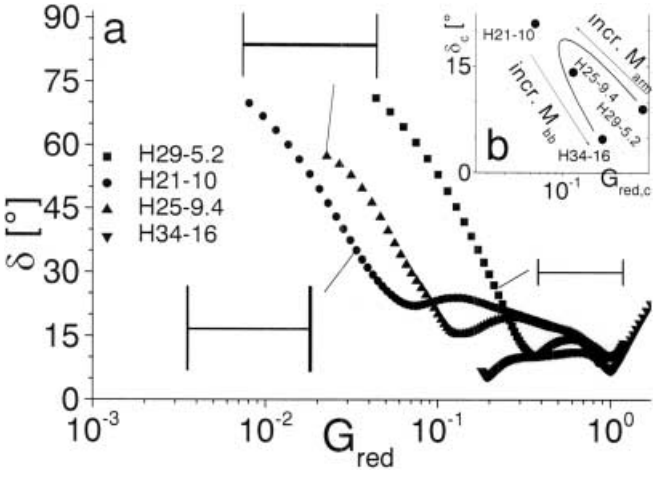

Fig. 5 a H-shaped poly(isoprene)s with various geometry ratios at 25 °C. The H sketches give an impression of the look of the molecule. **b** Location of points P_C, i.e., δ_c vs $G_{red,C}$

stars, almost no deviation from the linear behavior is found for the samples with small $s_{arm} \leq 1$. As the lengths of the arms increase, a bump develops due to a shift in balance between two different relaxation processes and the point P_c identifying the bump moves up left, passes a maximum, and drops down. There is no simple correlation between s_{arm} and the coordinates of P_c.

H-shaped polymers

H-shaped molecules differ from four-arm stars in the position of the branching points. Keeping the molecular weight constant, diverse topological variants are possible. If $s_{arm} >> s_{bb}$ then the molecule resembles a star. In case of $s_{arm} \approx s_{bb}$ one speaks of a ''regular'' H since the molecules remind one of the letter H. A stretched H is obtained when $s_{arm} << s_{bb}$. Here we analyze two sets of H-polymers. The rheological data of poly(isoprene)s with varied s_{arm} and s_{bb} ratios have been published by McLeish et al. (1999) and rheological measurements of some ''regular''-H poly(styrene)s have been performed by Roovers (1984). The important physical data and geometry ratio are captured in Tables 3 and 4 and the van Gurp-Palmen traces are shown in Figs. 5 and 6. The analysis of the characteristic points P_c reveals that δ_c of the Roovers H-polymers are higher than those of McLeish's, meaning the McLeish H-polymers are in general more elastic than the Roovers H-polymers. This is plausible since the molecular weights in units of M_e of the Roovers H-polymers are small compared to the McLeish H-polymers. The latter ones can be regarded as highly entangled. Within the Roovers series, P_c moves down left with increasing molecular weight. Lengthening the arms while keeping s_{bb} nearly constant results in a

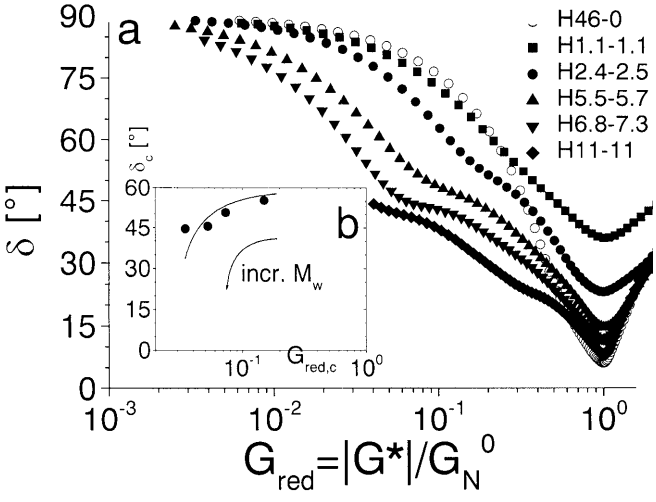

Fig. 6 a H-shaped poly(styrene)s at 169.5 °C by Roovers. The s_{bb}:s_{arm} ratio was kept constant and the arm lengths were stepwise increased. **b** Location of points P_C, i.e., δ_c vs $G_{red,C}$

shift of P_c towards lower $G_{red,c}$ and higher δ_c (compare H29–5.2 and H21–10; M_W of the arms are 110 kg/mol in both cases; the s_{arm}s in the coding are different, however, owing to McLeish's corrections). McLeish et al. (1999) explain this unexpected loss of elasticity, although the number of entanglements increase, with ''dynamic dilution''. This will be discussed below. The point P_c shifts down right with increasing s_{bb}. The McLeish and the Roovers series differ not only in the location of P_c but also in the distinct type of curve. While the Roovers H-polymers ''just'' show bumps similar to those of the stars, the McLeish H-polymers display developed min-

ima. We attribute a minimum at G_{red} values below 1 and low δ_c to a highly entangled state and regard the unique features of the curve, as given in Fig. 5, typical for entangled H-shaped molecules. A simple correlation between P_c and the structural parameters s_{arm} and s_{bb} could not be obtained.

Comb-polymers

Comb-polymers are distinguished from all other investigated polymers by a high number of side arms. The rheological data we present here (Figs. 7 and 8) have been published by Roovers and Graessley (1981). They investigated two series of comb-polymers with different backbone molecular weights and nearly constant number of branches (approximately 30 side arms per molecule). Within each row, the length of the side arms has been varied from 0 to $s_{arm} = 5.4$. The characteristic data are summarized in Table 5. Analogously to the star-polymers, one observes an almost linear rheological behavior for the samples with $s_{arm} < 1$. These curves have been omitted in Figs. 7 and 8 for clarity. When s_{arm} exceeds unity and the arms start to entangle, a bump forms at G_{red} values below 1. Increasing s_{arm} lowers $G_{red,c}$, raises δ_c, and the point P_c moves up left. Similar to the H-polymers, less elasticity, expressed by higher δ_c values, is against the expectation since longer side arms should be capable of entangling in a more pronounced way. As we will show below, dynamic dilution can explain this observation. Unique to comb-polymers are the correlations $\delta_c \propto \log G_{red,c}$ and $\delta_c \propto s_{arm}$ as well as the fact that the G_N^0 minima of the branched species are above the one of the neat backbone polymer. δ in the G_N^0 minimum drops with increasing arm length and therefore with increasing molecular weight.

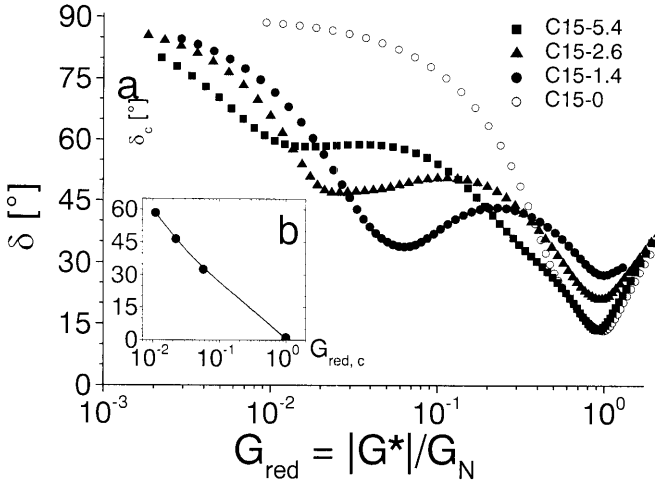

Fig. 7 a Comb-shaped poly(styrene)s with constant backbone (275 kg/mol) and increasing side arms lengths at 169.5 °C. Number of side arms was approximately 30 in all cases. **b** Location of points P_C, i.e., δ_c vs $G_{red,C}$

Comparison of H-, three-, and four-arm star-polymers

Figure 9 compares star- and H-polymers tallying in either s_{arm} or s_{total} ($s_{total} = s_{bb} + {}^{arms} \times s_{arm}$). Samples aS37–18 and sS38–19 have the same arm length and are very similar to one another with respect to the shape of the rvGP curve and the location of the corresponding points P_c although sS38–19 has an additional arm and thus a higher s_{total}. The same similarity is found for aS37–18 and sS29–14 where s_{total} is kept nearly constant. A significant difference is recognized, however, when

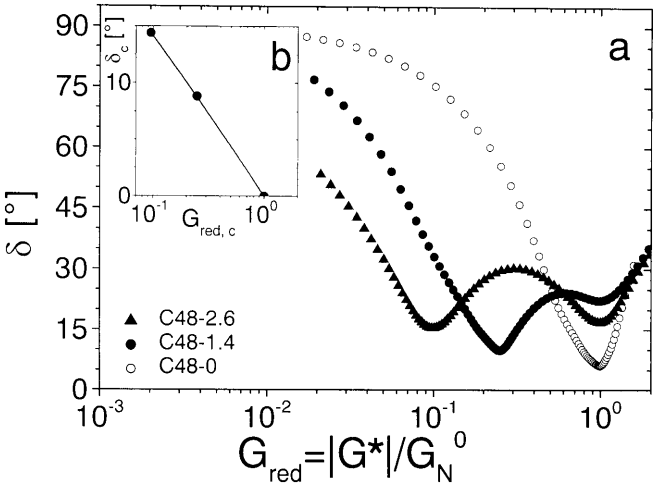

Fig. 8 a Comb-shaped poly(styrene)s with constant backbone (860 kg/mol) and increasing side arms lengths at 169.5 °C. Number of side arms was approximately 30 in all cases. **b** Location of points P_C, i.e., δ_c vs $G_{red,C}$

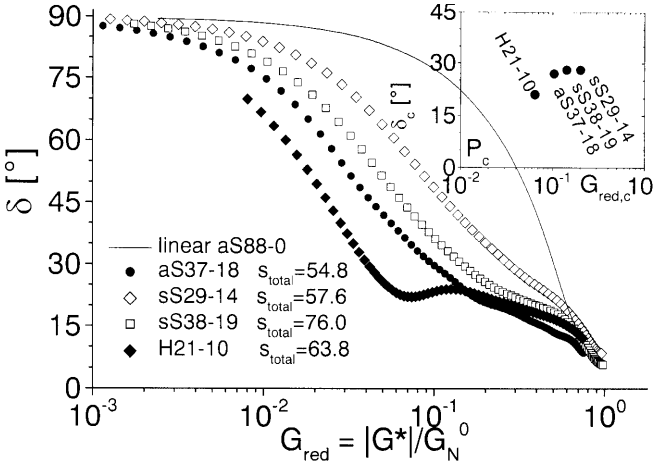

Fig. 9 Comparison of H-shaped, symmetric three- and four-arm star polymers at either constant s_{arm} or constant s_{total}

comparing the four-arm star sS29–14 with the H-polymer H21–10. Both samples have two arms and roughly the same s_{total} and differ only in distance between the two branching points. The δ_c values indicate that the H-polymer has a higher elasticity than the star-polymer. These findings lead to the conclusion that the rheological behavior of a sample is affected in a more pronounced manner by s_{bb} or the molecular weight between branching points than by the number of arms.

Topology-map

In Fig. 10 the points P_c of all probes under investigation are plotted in a single diagram. This way we phenomenologically obtain a chart that we call a topology map since certain topologies can preferably be found in specific regions on this map. Star-polymers are located in the sector defined and confined by the center C(10^0/0), the line through C and slope −30° per decade G_{red}, the curve for a linear monodisperse polymer and the segment around C through point (10^0/60°) – light gray area in Fig. 10. Highly entangled polymers, in particular stretched H-shaped polymers with $s_{bb} > 20$, gather in the sector defined by C, the abscissa, the straight line with slope –30° per decade G_{red} through point C, and the segment around C through point (4×10^{-2}/0°) – dark gray area. Diluted LCB polymers can be found in the ring section (striped area) that is defined by point C, the straight line through C with slope −30° per decade G_{red}, and the abscissa without considering the gray shaded areas.

"Dilution" can stand for real dilution, i.e., a polymer blend with a linear and a highly entangled LCB component (solid dots in Fig. 10, this blend series is discussed in detail below). It can also denote an idea

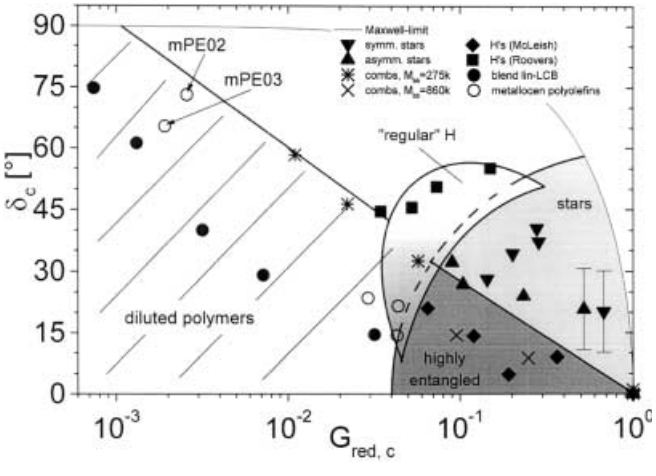

Fig. 10 Topology map. The points P_C characterizing the "bump" of LCB-polymers are plotted in one figure. Certain topologies can preferably be found in certain areas on the map

proposed by McLeish et al. (1999): the relaxation of a polymer chain with a long relaxation time will be accelerated by surrounding chains or chain segments with shorter relaxation times if these segments are already in the relaxed state. The relaxed elements surrounding the polymer chain are then efficiently acting as a diluent leading to a reduced overall elasticity. Applying this concept to comb-polymers one recognizes that the arms relax more rapidly than the entire chain does and therefore dilute the vicinity of the entire comb-molecule. With increasing arm length the volume fraction occupied by the arms (ϕ_{arm} in Table 5) grows and the dilution becomes more pronounced. This might explain why the points P_C of the comb series move up with increasing arm length.

The boundaries between the different areas are not sharp and the areas overlap to some extent. So, there exist H-shaped polymers with certain s_{arm} to s_{bb} ratios well above 1 that are located in the star sector since the shape of these H-polymers is very similar to those of stars. As the s_{arm} to s_{bb} ratio decreases, the character of the molecule changes from star-like to H-like. On the topology map, point P_c passes the corridor above/between the corresponding areas – gradually shaded sickle in Fig. 10 – and finally enters the sector of highly entangled polymers. As just illustrated, the areas on the topology map hold more than one topology class. We conclude that the topology map based on P_C, which is only a two parameter presentation of an entire curve, is not sufficient for the unambiguous characterization of an unknown sample. However, it can be utilized to exclude certain types of topologies, i.e., to reduce the number of possible topologies. For further delimiting, additional information or criteria are necessary. One possible source of information can be SEC diagrams. SEC, for example, can verify or rule out polymer mixtures. The course of the rvGP-curve can give precious hints on the topology of an unknown sample since each topology class features particular characteristics. In the following, a set of criteria is assigned to each topology class and only the combination of all features identifies this topology.

Star-polymers (i) The point P_C is found in the light gray shaded sector on the topology map. (ii) The rvGP curve carries three inflection points at G_{red} values below 1. The slopes of the tangent lines through these inflection points have the same sign. Pictorially speaking, the curve shows a bump without any minimum (see Figs. 3 and 4).

"Stretched" H-polymers (i) SEC excludes a polymer mixture of two linears with different molecular weight. (ii) The characteristic point P_C is located in the dark gray shaded sector on the topology map. (iii) In the rvGP-plot, there is a G_N^0 minimum at $G_{red} = 1$ (if experimentally accessible), another minimum at G_{red} below 1, and a short straight segment between these minima with constant slope (Fig. 5).

Comb-polymers Comb-polymers cannot be unambiguously identified. Especially the distinction from mixtures of linears and randomly branched polymers is hard to perform. Some of the features are as follows. (i) SEC excludes a polymer mixture of two linears with different molecular weight. (ii) The characteristic points P_C are located either in the striped ring section of diluted polymers on the topology map or in the dark gray shaded sector of highly entangled polymers. (iii) The vGP trace carries either a bump similar to those of star-polymers or a clearly developed minimum. In the latter case, comb-polymers can be differentiated from "stretched" H-polymers by the straight line/section in the rvGP curve between the G_N^0-region and minimum at G_{red}-values below 1. This straight section is typical for highly entangled H-shape polymers. (iv) The G_N^0-minimum of a comb-polymer is located at significant higher δ-values than the linear equivalent even if $M_W(comb) > M_w(lin)$ (see Figs. 7 and 8 in contrast to Figs. 12 and 9b of Trinkle and Friedrich 2001).

Mixtures LCB/linears Mixtures of LCB polymers and their linear analogue are discussed in detail below. This class of polymers features the following. (i) The characteristic point P_C is located in the striped ring section on the topology map. As stated in the previous section, mixtures of linears and randomly branched polymers are hard to separate from combs solely on basis of the vGP-plot. The synthesis condition might be able to rule out a comb-polymer. For example, a metallocene poly(ethene) with P_C in the striped ring section on the topology map is more likely to be a mixture than a comb-polymer since formation of a long chain branch is a statistical (Soares and Hamiliec 1996, 1997) rather than a controlled process.

Less defined polymers: metallocene poly(olefin)s

In the following sections we focus on ethene/propene copolymers, which were synthesized by means of metallocene catalysis (Table 6, Fig. 11). The reaction conditions, the used catalysts, and the accepted knowledge about the reaction mechanism do not exclude the formation of long chain branches (LCB). Further experimental observations are in agreement with the assumption of long chain branched polymers. (i) The time temperature superposition principle is not satisfactorily fulfilled (Fig. 1) which is a hint on LCB (Graessley 1982; Mavridis and Shroff 1992). (ii) The zero shear viscosities η_0 are significantly higher than expected from the $\eta_0 \propto M_w^{3.4}$ correlation. (iii) The rvGP-plots of these samples (Fig. 12a) deviate from the curves that are characteristic to linear polymers. A broad molecular weight distribution cannot account for this observation since the SEC analysis reveal polydispersity indexes around 2 and polydispersity does not change the character of curve anyway as evidenced by Fig. 2. Bimodality, i.e., a mixture of linears with different molecular weight (see Fig. 9 of Trinkle and Friedrich 2001) can be ruled out due to the monomodal SEC diagrams. A mixture of linears and LCB species having similar hydrodynamic volumina, however, remains possible.

Blends: linears and randomly branched polymers

In order to learn more about mixtures of linears and randomly branched polymers, such mixtures have been artificially produced by solution blending both components. As the LCB component mPE07 was chosen, a poly(ethene) whose characteristic point P_C is located in

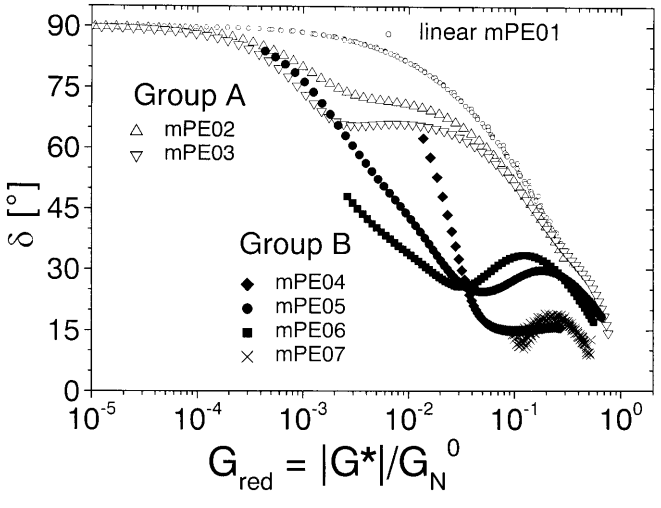

Fig. 11 Linear poly(styrene) and five long chain branched Metallocene-poly(olefin)s. The corresponding characteristic data are given in Table 6

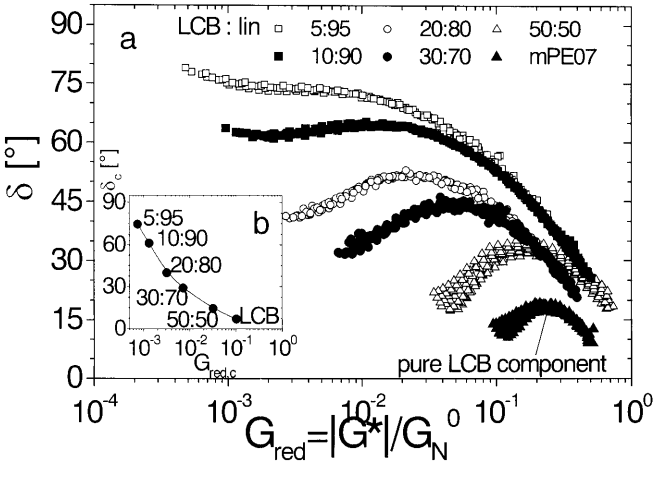

Fig. 12 a Mixtures of LCB-mPE07 and linear poly(ethene) at 170 °C. The compositions are given as weight fractions in percent. **b** Location of points P_C, i.e., δ_c vs $G_{red,C}$

the dark gray shaded sector on the topology map. The second component was a linear poly(ethene) of approximately the same polydispersity index. The corresponding rvGP-plots (Fig. 12) are like those of the linear/linear homopolymer blends (Trinkle and Friedrich 2001). The bumps, however, are more weakly developed than those of their linear/linear equivalents.

As explained above, the bump at G_{red} values below 1 which we attribute to the presence of long chain branching can be quantitatively described by a characteristic point P_C which is defined by the intersection of two tangent lines through the inflection points enclosing the bump. The analysis of point P_C reveals log $\delta_c \propto \log G_{red,c}$ and a linear correlation between log δ_c and the weight fraction of the LCB component ϕ_{LCB}. This enables one to asses the composition of an unknown linears/LCB blend. On the topology map the points P_C are found in the striped ring section of diluted polymers and with increasing fraction of linears, i.e., increasing dilution of LCB polymer with linears, P_C moves up left.

Characterization of mPE

In Fig. 12a three groups of polymers can be recognized: linear mPE01, group A-, and group B-polymers. Group A- and group B-polymers are distinguished in the location of the characteristic point P_C on the topology map. Group A-polymers are placed in the ring section of diluted polymers on the topology map (Fig. 10). Consequently, samples mPE02 and mPE03 cannot be star- or "regular" H-polymers nor highly entangled. They might be either combs-polymers of high functionality or mixtures of linears and LCB-molecules. The copolymerization tendency of the used catalyst (Walter 2000; Walter et al. 2001) indicates a statistical insertion of vinyl terminated macromers and thus a statistical distribution of long chain branches. So, it seems to be most probable that group A polymers are mixtures of linears and LCB components. By comparing the positions of P_C of these polymers with those of the artificially prepared mixture series, the composition of mPE02 and mPE03 can be roughly assessed to be in the range of 90 wt% linears. No further information can be given about the exact topology.

Group B-polymers can be found on the topology map in the overlap area between the sector of highly entangled resins and the ring section of diluted polymers. Therefore, a star-like topology can be excluded as well as "regular" and "stretched" Hs since the rvGP-traces do not exhibit the typical characteristics of H-polymers. More precise details about the topology and the branching frequency cannot be given as the copolymerization behavior of the used catalyst (MBI, Walter et al. 2001) cannot verify nor rule out the formation of comb-like polymers. If group B-polymers should happen to be mixtures of linears and LCB-molecules, the LCB fraction would be high.

Conclusion

The power of the reduced van Gurp-Palmen plot (rvGP) is the possibility to compare directly two polymers of different chemical nature. This is particularly important since only few model substances with ensured molecular topology are available. Substances need to be monodisperse and need to have polydispersity indices below ≈5 in order to be characterized by means of the rvGP-plot. In these cases, the point P_c of a branched probe can be reliably determined. Such a point P_C is a measure of the discrepancy from the behavior of a linear sample and depends on the polymer's topology. The two coordinates of P_C, i.e., $G_{red,c}$ and δ_c, mark a point on the so-called topology map spanned by the G_{red}- and the δ-axis. The conclusion of this work is that, while points P_C corresponding to a particular topology can be found predominantly in a limited area on the topology map, the reverse conclusion, that a point in a certain area on the topology map belongs unambiguously to one topology, turns out to be wrong. The reduction of the rvGP-"bump" to a single point or the reduction to the two parameters $G_{red,c}$ and δ_c is bound up with loss of information. Anyway, the topology map can be useful with an unknown sample to rule out some topologies and in combination with other sources of information like the rvGP curvature one can characterize this unknown sample with acceptable confidence. Information about the molecular weight distribution determined by SEC, the synthesis route, the catalysts, and the copolymerization parameters can also be of help. If it seems to be likely that an unknown sample is a mixture of linear and LCB species, the composition can be roughly assessed from the location of the point P_C. In agreement with other publications, our investigations revealed that the number of branches is less important for the rheological behavior than their position along the chain scaffolding.

Acknowledgments The authors are indebted to T.C.B. McLeish, H. Münstedt, and J. Roovers for committing some of their rheological data. K. Fuchs provided helpful advice and W. Fräßdorf searched the manuscript for mistakes. The *Graduiertenkolleg Strukturbildung in Makromolekularen Systemen* funded this work.

References

Donth EJ (1992) Relaxation and thermodynamics in polymers. Akademie Verlag, Berlin, p 22

Eckstein A, Suhm J, Friedrich C, Maier RD, Sassmannshausen J, Bochmann M, Mülhaupt R (1998) Determination of plateau moduli and entanglement molecular weights of isotactic, syndiotactic and atactic polypropylenes synthesized with metallocene catalysts. Macromolecules 31:1335–1340

Fetters LJ, Kiss AD, Pearson DS, Quack GF, Vitus FJ (1993) Rheological behavior of star-shaped polymers. Macromolecules 26:647–654

Gabriel C, Münstedt H (1999) Creep recovery behavior of metallocene linear low-density polyethylenes. Rheol Acta 38:393–405

Gell CB, Graessley WW, Fetters LJ (1997a) Viscoelasticity and self-diffusion in melts of entangled linear polymers. J Polym Sci Polym Phys Ed 35:1933–1942

Gell CB, Graessley WW, Efstratiadis V, Pitsikalis M, Hadjichristidis N (1997b) Viscoelasticity and self-diffusion in melts of entangled asymmetric star polymers. J Polym Sci Polym Phys Ed 35:1943–1954

Graessley WW (1982) Effect of long chain branches on the temperature dependence of viscoelastic properties in polymer melts. Macromolecules 15:1164–1167

Honerkamp J, Weese J (1993a) A note on estimating mastercurves. Rheol Acta 32:57–64

Honerkamp J, Weese J (1993b) A nonlinear regularization method for the calculation of relaxation spectra. Rheol Acta 32:65–73

Janzen J, Colby RH (1999) Diagnosing long-chain branching in polyethylenes. J Mol Struct 485/486:569–584

Lai S, Plumley TA, Butler TI, Knight GW, Kao CI (1994) Dow rheology index (DRI) for insite technology polyolefins (ITP): unique structure-processing relationships. SPE ANTEC 94:1814–1815

Mavridis H, Shroff RN (1992) Temperature dependence of polyolefin melt rheology. Polym Eng Sci 32:1778–1791

McLeish TCB, Allgaier J, Bick DK, Bishko G, Biswas P, Blackwell R, Blottière B, Clarke N, Gibbs B, Groves DJ, Hakiki A, Heenan RK, Johnson JM, Kant R, Rad DJ, Young RN (1999) Dynamics of entangled H-polymers: theory, rheology and neutron-scattering. Macromolecules 32:6734–6758

Roovers J (1979) Synthesis and dilute characterization of comb polystyrenes. Polymer 20:843–849

Roovers J (1984) Melt rheology of H-shaped polystyrenes. Macromolecules 17:1196–1200

Roovers J, Graessley WW (1981) Melt rheology of some model comb polystyrenes. Macromolecules 14:766–773

Roovers J, Toporowski PM (1981) Preparation and characterization of H-shaped polystyrenes. Macromolecules 14:1174–1178

Seo Y, Ung Kim K (1994) A new model for rapid evaluation of the degree of long-chain branching in polymers. Polymer 35:4163–4167

Shaw MT, Tuminello WH (1994) A closer look at the MWD-viscosity transform. Polym Eng Sci 34:159–165

Shroff RN, Mavridis H (1999) Long-chain branching index for essentially linear polyethylenes. Macromolecules 32:8454–8464

Soares JBP, Hamielec AE (1996) Bivariate chain length and long chain branching distribution for copolymerization of olefins and polyolefin chains containing terminal double bonds. Macromol Theory Simul 5:547–572

Soares JBP, Hamielec AE (1997) The chemical composition component of the distribution of chain length and long chain branching for copolymerization of olefins and polyolefin chains containing terminal double-bonds. Macromol Theory Simul 6:591–596

Suhm J (1998) PhD Thesis, University of Freiburg

Trinkle S, Friedrich C (2001) Van Gurp-Palmen-plot: a way to characterize polydispersity of linear polymers. Rheol Acta 40:322–328

van Gurp M, Palmen J (1998) Time-temperature superposition for polymeric blends. Rheol Bull 67:5–8

Vega JF, Santamaria A (1998) Small-amplitude oscillatory shear flow measurements as a tool to detect very low amounts of long chain branching in polyethylenes. Macromolecules 31:3639–3647

Walter P (2000) PhD Thesis, University of Freiburg

Walter P, Trinkle S, Mülhaupt R (2001) Influence of zirconocene structure and propene content on melt rheology of polyethene and ethene/propene copolymers. Polym Bull (accepted)

Wood-Adams PM, Dealy JM (1996) Use of rheological measurements to estimate the molecular weight distribution of linear polyethylene. J Rheol 40:761–778

Wood-Adams PM, Dealy JM (2000) Using rheological data to determine the branching level in metallocene polyethylenes. Macromolecules 33:7481–7488

Wood-Adams PM, Dealy JM, deGroot W, Redwine OD (2000) Effect of molecular structure on the linear viscoelastic behavior of polyethylene. Macromolecules 33:7489–7499